Self-Similar Magnetoresistance of a Semiconductor Sinai Billiard

R. P. Taylor,[1,2] R. Newbury,[1,2] A. S. Sachrajda,[1] Y. Feng,[1] P. T. Coleridge,[1] C. Dettmann,[2]
Ningjia Zhu,[3] Hong Guo,[3] A. Delage,[1] P. J. Kelly,[1] and Z. Wasilewski[1]
[1]*I.M.S., National Research Council, Ottawa, KIA OR6, Canada*
[2]*School of Physics, University of New South Wales, Sydney, 2052, Australia*
[3]*Department of Physics, McGill University, Montreal, H3A 2T8, Canada*
(Received 1 July 1996)

We investigate the transition to a Sinai geometry by introducing a circular pattern at the center of a square mesoscopic billiard defined in a high quality AlGaAs/GaAs crystal. The transition induces a novel quantum interference structure in the magnetoresistance with a characteristic field scale over an order of magnitude smaller than previously reported in mesoscopic billiards. A systematic comparison of fine and coarse structures, which differ by an order of magnitude in field scale, demonstrates the first observation of geometry-induced "self-similarity" in the magnetoresistance of a semiconductor system. [S0031-9007(97)02544-1]

PACS numbers: 72.20.My, 05.45.+b, 73.20.Dx, 73.20.Fz

Quantum interference phenomena such as weak localization (WL) and aperiodic conductance fluctuations (ACF) can be viewed as "magneto-fingerprints" of the mesoscopic scattering processes determining electronic transport in semiconductors and metal films [1,2]. At low temperatures, electron phase coherence is maintained over large distances and a semiclassical analysis involves monitoring the phase accumulated by electrons as they move along classical trajectories shaped by elastic scattering events. Quantum interference processes then result from pairs of trajectories which form closed loops, and are sensitive to the distribution of enclosed areas. Originally observed in disordered systems, improvements in semiconductor growth and device fabrication have led to the realization of cavities smaller than the average impurity spacing, and studies of WL and ACF have found a new role as a probe of "quantum chaos." For these "billiards," at low temperatures large angle scattering occurs predominantly at the device boundaries so that distinctly different characteristics are expected for idealized cavity geometries which generate regular or chaotic scattering of the classical electron trajectories [3]. Differences in the quantum behavior were investigated in experiments performed on circular (regular) and stadium (chaotic) shaped billiards. Analysis of the power spectrum of the ACF [4] and the line shape of the WL peak [5] observed in the low field magnetoresistance confirmed the predicted relationships between quantum behavior and classical scattering dynamics. This link has also recently been explored in resonant tunneling diodes [6] and antidot superlattices [7].

In this Letter, we investigate the transition to a Sinai geometry by introducing a circular pattern at the center of a square billiard. For a system described by hard-wall profiles, the convex surface of the circular scatterer acts as a "Sinai diffuser" producing exponentially diverging classical trajectories [8], in sharp contrast to the regular dynamics supported by the empty square. As the size of the circle is increased, the rate at which trajectories interact with the Sinai diffuser before escaping through the leads increases: In this way the Lyapunov exponent describing the system [9] can effectively be tuned. For a physical system, such as a semiconductor billiard, the exact character of the profiles defining the geometry is important. Departures from strict hard-wall profiles for the Sinai diffuser may lead to a mixed (regular and chaotic) classical phase space, as found for other systems [7,10,11]. The nature of the square-Sinai geometry evolution is of fundamental interest. Furthermore, the ability to induce a distinct geometry change within a single device offers a comparatively unambiguous result—comparisons of two devices featuring different geometries [4,5] are potentially restrictive as, for a physical system, variations attributed to geometry must be separated from other changing parameters, in particular, those related to the host material. We will show that, during this novel transition, quantum interference structure emerges in the magnetoresistance with a characteristic magnetic field scale over an order of magnitude smaller than that reported in previous studies of mesoscopic billiards with significantly lower electron mobilities [4,5]. Furthermore, this structure exhibits a striking similarity to structure observed on a coarser magnetic field scale. This first experimental observation of geometry-induced "self-similarity" in the magnetoresistance has important implications for the relationship between quantum interference processes and the classical phase space realized in a semiconductor billiard: Fractal behavior has recently been predicted in the ACF for mixed classical phase space [10].

The device configuration is shown in the insets to Fig. 1. Three "outer" electrostatic gates deposited on the surface of an AlGaAs/GaAs heterostructure form a 1 μm square with 0.2 μm wide entrance and exit leads. This square is significantly smaller than the 25 μm mean free path (l_e) but larger than the 0.05 μm Fermi wavelength (corresponding to an electron density of 2.3×10^{15} m^{-2}) of the two-dimensional electron gas (2DEG) located

 0031-9007/97/78(10)/1952(4)$10.00

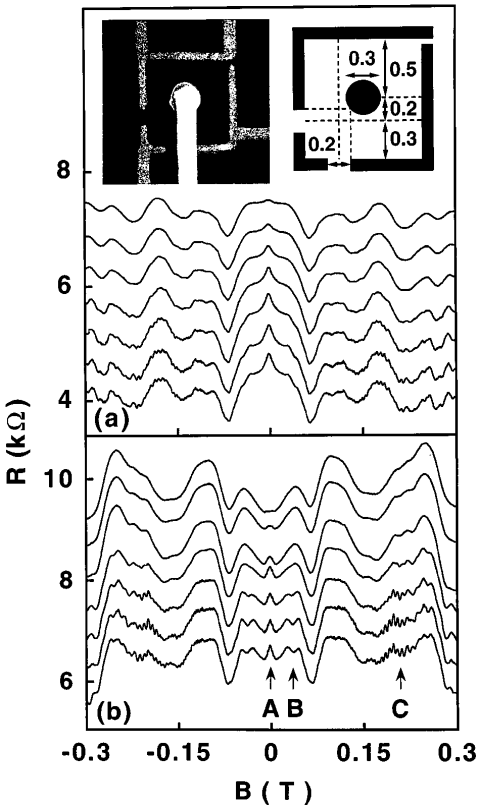

FIG. 1. Magnetoresistance of the square (a) and the Sinai billiard (b) for the temperatures 30 mK (bottom), 0.1, 0.4, 0.8, 1.6, 2.5, and 3.3 K (top). $V_0 = -0.52$ V. See text for the labels *A*, *B*, and *C*. The insets show a scanning electron micrograph and dimensions of the device.

103 nm below the semiconductor surface. The "inner" circular gate (with a diameter 0.3 μm) is connected by a bridging interconnect [12] and biased at the voltage V_I. The potential profiles defined in the 2DEG are not affected by the interconnect itself [12]. By applying a negative bias V_0 to the outer gates to define the square, we evolve the device geometry by tuning V_I. For $V_I = +0.7$ V, the presence of the central gate is minimized [13]. As the positive bias is reduced, the region under the gate becomes partially depleted, followed by full depletion at $V_I = 0$ V, at which point the associated antidot at the center of the square changes the device geometry to a Sinai billiard. The radius R of the channel formed around the antidot is estimated to increase linearly with approximate increments of $\Delta R \approx +40$ nm for $\Delta V_I \approx -0.5$ V (see below) [12]. The maximum bias of -3.3 V is determined by gate leakage current considerations. The conducting channel around the antidot can be further narrowed by an increase in the negative bias V_0 and, as the channel approaches pinch-off, the device geometry evolves beyond a Sinai billiard description. Further characterization details will be presented elsewhere.

Classical and quantum contributions to the magnetoresistance can be distinguished using the temperature dependences of the square ($V_I = +0.7$ V) and Sinai ($V_I = -3$ V) billiards shown in Figs. 1(a) and 1(b), respectively. Classical features, seen in the high temperature magnetoresistance ($T = 3.3$ K, top traces), are used to monitor the evolution of the electron trajectories as the antidot is formed. General characteristics of the 3.3 K traces are confirmed by a classical trajectory analysis used previously to successfully model circular billiards [14]. In particular, we note that for the square billiard the resistance maximum at zero field is due to reflection of trajectories from the far wall back into the entrance lead. In contrast, the Sinai billiard has a minimum at zero field because a number of trajectories hit the antidot and are focused into the exit lead. The features marked *A* to *C* in Fig. 1 are absent from the classical analysis and exhibit a sharper temperature dependence than expected classically [13–15], indicating a quantum mechanical origin. The structure marked *C* is matched to the Shubnikov-de Haas oscillations in the bulk 2DEG. Feature *A* is a weak localization peak, and its full width at half maximum ($\Delta B_{\mathrm{FWHM}} \approx 10$ mT) is confirmed for our Sinai billiard by solving the Schrödinger equation using the finite-element numerical scheme described elsewhere [16]. Approximating the characteristic trajectory loop area A using the equation $\Delta B_{\mathrm{FWHM}} = h/2\pi eA$ [4], the WL process involves loop areas substantially smaller than the cavity, as has recently been reported in other devices [13,17]. The structure marked *B* emerges as the antidot is formed and is strikingly different to typical ACF seen in devices with smaller l_e [4,18] (2–5 μm compared to our system's 25 μm). Evidence for conductance fluctuations which are periodic in magnetic field has been seen in other billiards [4,5,19] and attributed to unstable periodic orbits. If we interpret the structure as oscillations which are periodic in magnetic field, and apply the magnetic flux relationship $\Delta B = \phi_0/A$ (where $\phi_0 = h/e$) to the magnetic field period ΔB, assuming a circular trajectory for the loop area A, the corresponding radius R is physically reasonable: 0.32 μm for $V_I = -3.0$ V. However, by fine tuning V_I and V_0 the amplitudes of neighboring maxima are shown to evolve independently (see later), and an alternative picture of distinct resistance peaks is appropriate.

Figure 2 shows the evolution of the classical and quantum structure as the device undergoes the transition from square ($V_I = +0.7$ V, bottom trace) to Sinai billiard ($V_I = -2.9$ V, top trace) for a fixed V_0 and a lattice temperature of $T = 30$ mK. The initial sharp rise in background resistance observed as V_I is changed is associated with the formation of the antidot, followed by a more gradual increase as the antidot radius increases. A close inspection of the WL peak reveals the fine scale structure shown in Fig. 3. Features on this fine magnetic field scale have not previously been reported for billiards. The temperature dependence of the fine structure, shown in Fig. 4, implies a quantum mechanical origin. For both the Sinai and square billiards, the conductance amplitude ΔG_F of the fine central peak decreases exponentially with increasing temperature, consistent with recent studies of WL processes in billiards [13,18]. The conductance

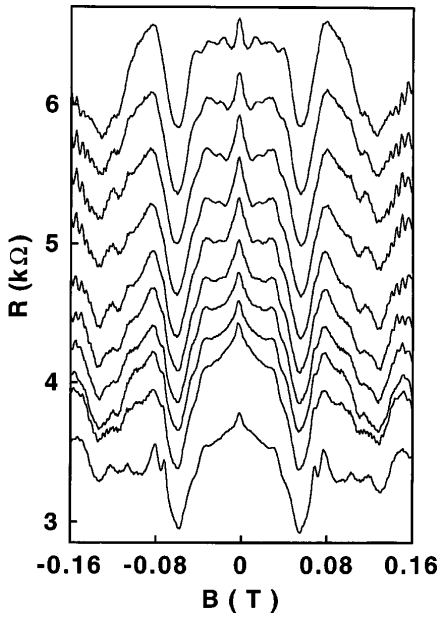

FIG. 2. The magnetoresistance showing the transition from a square (bottom trace, $V_I = +0.7$ V) to Sinai billiard (top trace, $V_I = -2.9$ V). The intermediate traces have an increment of 0.4 V in V_I. $T = 30$ mK. $V_0 = -0.51$ V.

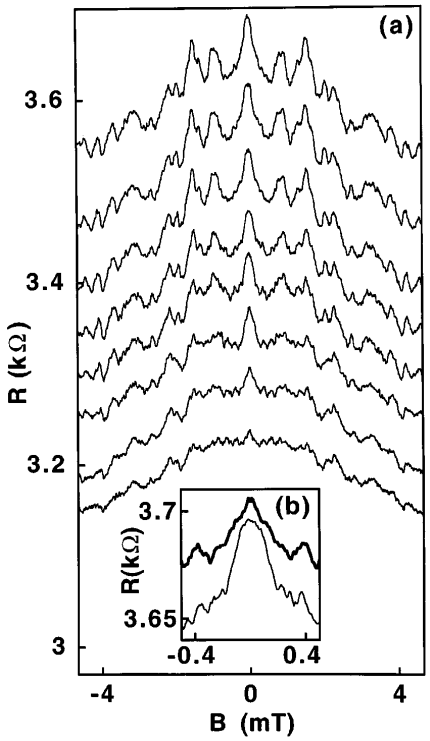

FIG. 3. (a) The fine structure as a function of V_I. $T = 30$ mK, $V_0 = -0.51$ V. The traces are vertically offset for clarity. From the bottom, the V_I and R_0 values are $(+0.7\text{ V}, 3.24\text{ k}\Omega)$, $(+0.3\text{ V}, 3.71\text{ k}\Omega)$, $(-0.7\text{ V}, 4.1\text{ k}\Omega)$, $(-1.9\text{ V}, 4.96\text{ k}\Omega)$, $(-2.3\text{ V}, 5.26\text{ k}\Omega)$, $(-2.7\text{ V}, 5.58\text{ k}\Omega)$, $(-2.9\text{ V}, 5.72\text{ k}\Omega)$, and $(-3.3\text{ V}, 6.05\text{ k}\Omega)$. (b) The $V_I = -2.3$ V (fine) trace approximately vertically aligned to the $V_I = +0.3$ V (bold) trace to facilitate a comparison of the line shapes of the fine central peak.

amplitude of the fine structure increases as the channel around the antidot is formed, consistent with quantum interference of trajectories shaped by the channel within the Sinai geometry. Furthermore, if V_0 is now increased and the channel approaches pinch-off, a decrease in conductance amplitude is observed for all fine structure features (note, because the background resistance R increases significantly as V_0 is increased, a decrease in conductance amplitude ΔG produces an increase in resistance amplitude ΔR for certain features because $\Delta R = -\Delta G R^2$. See later). The conductance amplitudes of the individual features evolve independently as V_0 is increased, with the narrow central resistance peak decreasing most dramatically. We attribute this peak ($\Delta B_{\text{FWHM}} = 0.3$ mT) to a second WL process. Using $\Delta B_{\text{FWHM}} = h/2\pi eA$, the calculated typical loop area is twice that of the lithographic square, corresponding to multiple orbits of the billiard. Such long trajectories sample all features of the device geometry, and the line shape of the WL peak would be expected to change from linear (regular) to Lorentzian (chaotic) [5] as the device geometry evolves from a square to a Sinai billiard. Figure 3(b) shows the observed change in line shape.

The remarkable similarity of the "magneto-fingerprints" observed over the coarse (Fig. 2) and fine (Fig. 3) magnetic field scales for the Sinai billiard is explored further in Fig. 5. Figure 5(a) details the fine structure observed on top of the coarse WL peak shown in Fig. 5(b). The two pictures have been scaled such that the widths of the fine and coarse WL peaks are approximately the same. Both field ranges exhibit a WL peak and a set of quasiperiodic, independent peaks which emerge on formation of the Sinai billiard. Figures 5(c) and 5(d) and 5(e) and 5(f) show the corresponding pairs of traces as V_0 is made more negative. The evolution of the fine structure follows closely that observed on the coarse scale, suggesting a novel self-similarity in the magnetoresistance [20]. To quantify these observations, we estimate the fractal dimension [21] for the pair of traces as $D \approx 2 - [\ln(\Delta R_C/\Delta R_F)/\ln(\Delta B_C/\Delta B_F)]$, where ΔR_F and ΔR_C are the amplitudes of the fine and coarse features. ΔB_F and ΔB_C are the corresponding magnetic field scales. A comparison of the WL peaks in Figs. 5(a) and 5(b) gives $D \approx 1.5$. Given that ΔB is inversely proportional to A, the expression for D implies that over the experimentally observed scales $\Delta R \propto A^{-\gamma}$, where $\gamma = 2 - D \approx 0.5$. The trajectory lengths corresponding to the observed values of ΔB are of the order of 1–10 μm and are not therefore predominantly affected by phase-breaking scattering events (assuming the phase coherence length to be significantly larger than the l_e value of 25 μm [18,22]). However, the trajectory lengths are comparable to the calculated typical dwell length within the billiard of 10 μm [16], which therefore determines the distribution of loop perimeters. This suggests a possible explanation for the relative scaling of the features: ΔR is proportional to the number of quantum interference loops confined in the billiard, which for generic chaotic systems is expected to obey a power law

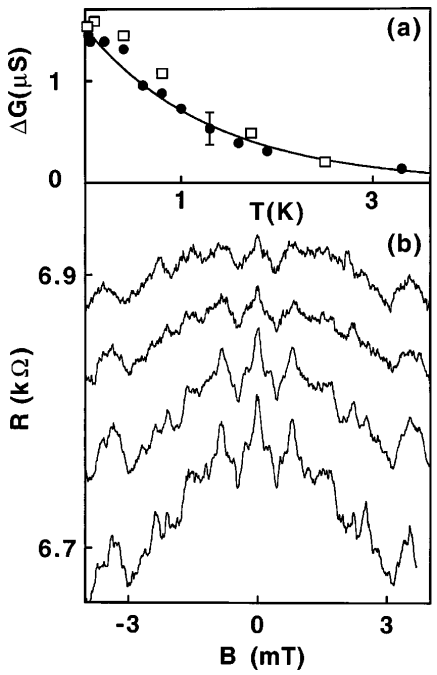

FIG. 4. (a) Exponential temperature dependence of the conductance amplitude ΔG of the fine WL resistance peaks for the Sinai ($V_I = -2.8$ V, $V_0 = -0.52$ V, circles) and square ($V_I = +0.7$ V, $V_0 = -0.51$ V, squares) billiards. (b) Fine magnetoresistance structure for the Sinai billiard ($V_I = -2.8$ V). The temperatures and ($B = 0$ T) resistances are (0.03 K, 6.81 kΩ, bottom), (0.8 K, 7.42 kΩ), (1.6 K, 8.61 kΩ), and (1.9 K, 8.64 kΩ).

dependence on A [10]. Within this picture, it is important to establish the range of ΔB for which self-similar structure can be experimentally observed. The largest scale is limited to magnetic fields significantly below that at which the cyclotron radius matches the device size ($\approx$150 mT).

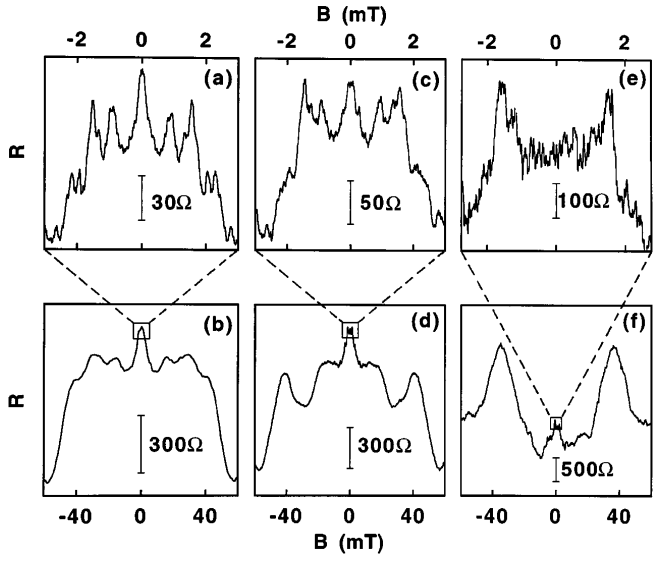

FIG. 5. "Fine" structure (a), (c), (e) and corresponding "coarse" structure (b), (d), (f) observed for the Sinai billiard ($V_I = -2.7$ V). $T = 30$ mK. The V_0 and ($B = 0$ T) resistances are (a), (b) -0.51 V, 4.8 kΩ, (c), (d) -0.52 V, 7.5 kΩ, and (e), (f) -0.55 V, 22 kΩ.

The smallest scale is set by the capability to resolve the value of ΔR calculated from D: When we examine the fine WL peak, we see remnants of structure at an even finer scale, with a characteristic peak width of 0.03 mT. The expected amplitude estimated from D for this field scale is 14 Ω, of a similar order to the observed value of 5 Ω. This indicates the possibility of a third hierarchy of self-similarity, although experimental resolution limits a clear identification to two field scales. Finally, we note that fractal magnetoresistance behavior has been recently predicted for mixed (chaotic and regular) classical phase space [10]. It was shown that for billiards defined by parabolic potentials, a self-similar phase space structure containing a hierarchy of cantori, produces fractal behavior in the ACF. The fascinating quality of the self-similar behavior observed in our experiments is that the magnetofingerprint is not a rich spectrum of ACF patterns but very distinct WL peaks and quasiperiodic structure.

We thank J. P. Bird, T. M. Fromhold, and G. Morriss for helpful discussions.

[1] G. Bergmann, Phys. Rep. **107**, 1 (1984).
[2] P. A. Lee and A. D. Stone, Phys. Rev. Lett. **55**, 1622 (1985).
[3] R. A. Jalabert, H. U. Baranger, and A. D. Stone, Phys. Rev. Lett. **63**, 2442 (1989); H. U. Baranger, R. A. Jalabert, and A. D. Stone, Phys. Rev. Lett. **70**, 3876 (1993).
[4] C. M. Marcus *et al.*, Phys. Rev. Lett. **69**, 506 (1992).
[5] A. M. Chang *et al.*, Phys. Rev. Lett. **73**, 2111 (1994).
[6] T. M. Fromhold *et al.*, Phys. Rev. Lett. **75**, 1142 (1995).
[7] R. Fleischmann, T. Geisel, and R. Ketzmerick, Phys. Rev. Lett. **68**, 1367 (1992).
[8] Ya G. Sinai, Russ. Math. Survey **25**, 137 (1970).
[9] R. V. Jensen, Chaos **1**, 101 (1991).
[10] R. Ketzmerick, Report No. cond-mat/9510007 [Phys. Rev. B (to be published)].
[11] E. Ott, *Chaos in Dynamical Systems* (Cambridge University Press, Cambridge, 1993), p. 260.
[12] A. S. Sachrajda *et al.*, Phys. Rev. B **50**, 10 856 (1994).
[13] R. P. Taylor *et al.*, Phys. Rev. B **51**, 9801 (1995); Semi. Sci. Technol. **11**, 1 (1996).
[14] R. P. Taylor *et al.*, Solid State Commun. **87**, 579 (1994); Phys. Rev. B **47**, 4458 (1993).
[15] J. Spector *et al.*, Appl. Phys. Lett. **56**, 967 (1990).
[16] Y. Wang, J. Wang, and H. Guo, Phys. Rev. B **49**, 1928 (1994).
[17] G. Lutjering, K. Richter, D. Weiss, J. Mao, R. H. Blick, K. v. Klitzing, and C. T. Foxon, Surf. Sci. (to be published).
[18] J. P. Bird *et al.*, Phys. Rev. B **42**, R14 336 (1990); Phys. Rev. B **51**, R18 037 (1995).
[19] J. P. Bird *et al.*, Europhys. Lett. **35**, 529 (1996).
[20] The emergence of self-similarity during the transition from the square to the Sinai billiard has been observed in an ensemble of 150 billiards with distinct geometries corresponding to different inner and outer gate biases.
[21] B. B. Mandelbrot, *The Fractal Geometry of Nature* (Freeman, San Francisco, 1982).
[22] R. M. Clarke *et al.*, Phys. Rev. B **52**, 2656 (1995).